

NISTIR 6963

Standard Reference Photometer for the Assay of Ozone in Calibration Atmospheres

R.J. Paur, A.M. Bass, J.E. Norris, and T.J. Buckley

QC
100
.456
#6963
2003

NIST

National Institute of Standards and Technology
Technology Administration, U.S. Department of Commerce

NISTIR 6963

Standard Reference Photometer for the Assay of Ozone in Calibration Atmospheres

Richard J. Paur

*United States Army Research Office
Army Research Office
Research Triangle Park, NC 27709*

***Arnold M. Bass**

James E. Norris

****Thomas J. Buckley**

*Chemical Science and Technology Laboratory
National Institute of Standards and Technology
Gaithersburg, MD 20899*

** Deceased*

*** Formerly of NIST*

February 2003



U.S. DEPARTMENT OF COMMERCE

Donald L. Evans, Secretary

TECHNOLOGY ADMINISTRATION

Phillip J. Bond, Under Secretary of Commerce for Technology

NATIONAL INSTITUTE OF STANDARDS AND TECHNOLOGY

Arden L. Bement, Jr., Director

ABSTRACT.....	6
1. INTRODUCTION.....	7
2. PERFORMANCE SPECIFICATIONS	7
3. MEASUREMENT PRINCIPLE	7
4. DESIGN	8
5. ELECTRONICS OPERATION	8
6. GAS FLOW and OZONE GENERATION	9
7. MATERIALS and DIMENSIONS.....	9
8. PHOTOMETRIC MEASUREMENTS WITH THE SRP	9
9. PERFORMANCE	11
10. ANALYSIS OF PERFORMANCE	12
11. MEASUREMENT UNCERTAINTIES.....	14
12. CONCLUSIONS.....	15
13. ACKNOWLEDGEMENTS	15
14. REFERENCES	16

ABSTRACT

A photometric instrument for the assay of ozone from 0 ppbv to 1000 ppbv in calibration atmospheres has been designed, constructed, and evaluated. The absorption cross-section of ozone at 254 nm (Hg line) is the major component of uncertainty of the instrument. A number of workers have determined this cross-section to be about $1.147 \times 10^{-17} \text{ cm}^2/\text{molecule}$ (or equivalently $308.32 \text{ atm}^{-1} \text{ cm}^{-1}$, base e), with a standard uncertainty of 1.0 %. To a lesser extent, the uncertainty of the instrument also depends on the uncertainty of the temperature, pressure, and transmittance measurements on the ozone sample. Based upon ozone calibration needs of the U.S. EPA, the design specifications called for an instrument with a standard uncertainty of 2 ppbv in the range of 1 ppbv to 100 ppbv and 2 % in the range of 100 ppbv to 1000 ppbv.

Thirty-one of these instruments, called Standard Reference Photometers (SRP), have been built since 1983; each SRP has met or exceeded the design specifications. Two of these instruments are maintained at the National Institute of Standards and Technology (NIST), one serving as NIST's principal ozone standard, and the other serving as a backup and quality system check instrument. Ten additional instruments of the same design are maintained at various EPA or state operated laboratories across the United States to facilitate local access to authoritative ozone standards. The current network of SRPs also includes instruments maintained in Australia, Austria, Canada, the Czech Republic, France, Germany, Portugal, Spain, Switzerland, Sweden, Taiwan R.O.C. and the United Kingdom. Each of the SRPs provides ozone assays with a certified uncertainty similar to that of a Standard Reference Material (SRM) obtained from NIST.

1. INTRODUCTION

During the period 1974-1978 the EPA carried out a program to evaluate methods for the generation and assay of ozone atmospheres to calibrate air monitoring instruments used to measure the ozone content of ambient air. As a result of this program, the previously used method (a 1% buffered potassium iodide titration method) specified in the US EPA Federal Reference Method (FRM) (1) for ozone was replaced with an ultraviolet photometry technique for improved accuracy, robustness, and ease of operation. The FRM provided performance specifications for a UV photometric instrument and offered detailed technical guidance to enable commercial development of photometers that would meet the new assay procedure requirements. A number of manufacturers began marketing instruments that would meet the required specifications.

Members of the user community responsible for the traceability of calibration standards are frequently faced with the task of verifying that a given ozone photometer does in fact meet all performance specifications. To provide an easily implemented program for verification of ozone standards, the EPA and the National Bureau of Standards, now the National Institute of Standards and Technology (NIST), undertook to design, construct, certify, and deploy a network of Standard Reference Photometers (SRP) for the assay of ozone. Table 1 shows the current network of SRPs, their locations, and Organization.

The design and performance of the SRP is the subject of this paper.

2. PERFORMANCE SPECIFICATIONS

To meet the EPA's regulatory needs for an authoritative ozone standard, the SRP was designed to measure ozone with a standard uncertainty of 5.0×10^{10} molecules/cm³ (2 ppbv¹-parts per billion, by volume, 10⁹) at Standard Temperature and Pressure (STP = 273.15 K and 101.3 kPa) in the range of 0 - 2.5×10^{12} molecules/cm³ (0-100 ppbv) and 2% in the range of 2.5×10^{12} molecules/cm³ - 2.5×10^{13} molecules/cm³ (100-1000 ppbv).

3. MEASUREMENT PRINCIPLE

The basic measurement principle of the SRP is the determination of the amount of ultraviolet radiation at a specific wavelength (253.7 nm mercury line) absorbed by a sample of ozonized air. From the transmittance of the radiation through the sample, the ozone content of the sample is determined by the application of the Beer-Lambert Law. The accurate determination of the transmittance requires that care be taken to avoid errors caused by stray radiation and sample and light source variations during the course of the measurement. The sample temperature and pressure are also measured to allow for correction of the ozone concentration to standard conditions using the ideal gas law. Typically, ozone is generated by the photolysis of purified air using radiation at 185 nm. The purified zero air, now referred to as "reference air", is assumed to contain no significant impurities, have less than 1000 ppbv total hydrocarbons, and contain 20 - 21% oxygen. Reference air adequate for this application is obtainable in cylinders through commercial suppliers or compressed air filtered through appropriate purification

¹ Because the unit of ppbv is most commonly used in ozone calibration work, it will hereafter exclusively be used in this paper.

materials such as silica gel, activated charcoal, and molecular sieves. Tests conducted between commercial and in-house reference air showed no differences between them in this application.

4. DESIGN

The concept for the optical design, the gas flow system, and the data processing was developed in 1976 as a result of an effort to develop an instrument suitable for the measurement of ozone in aircraft cabins. A study of the proposed design indicated that a highly precise instrument could be made that minimized the requirements for linearity of the detector, preamplifier, and digitizer. The design is based on a pair of identical absorption cells; one serves as the sample cell and the other serves as the reference cell. Using a control system (described later in detail), each optical cell alternates between sample and reference during an instrument cycle. An instrument based on this principle was independently designed and constructed by Proffitt (2), and was used successfully in balloon-borne and aircraft measurements of stratospheric ozone.

The basic layout of the SRP is shown in Figure 1. The SRP is a modular instrument consisting of an optical bench assembly, an electronics control and signal conditioning unit, a pneumatics and ozone generator unit, and a data acquisition, processing, display, and storage system (computer).

5. ELECTRONICS OPERATION

The electronics control and signal conditioning unit or "Electronics Module" consists of power supplies and signal processing/interface circuitry. The Electronics Module is connected to a control computer through a cable connection on the rear panel. The computer has direct control of the solenoid valves, the lamp shutter, and the electronic counters (scalers) through a digital Input/Output (I/O) interface card. This provides flexibility in the various SRP operating modes. The operating modes differ only in the sequence of execution of programmable commands.

Data generated by the SRP consists of four frequencies that are digitized by individual counter circuits. These frequencies, shown in Figure 2, are generated by independent voltage to frequency converters for the temperature, pressure, detector 1, and detector 2 signals. The count values are read from the scaler circuits by the control computer in a BCD digit serial fashion. The temperature signal is produced by a commercial electronic thermometer using a platinum temperature sensor (RTD) with an inaccuracy stated by the manufacturer (traceable to NIST) within 0.2% of the temperature reading plus ± 0.1 °C of that value (i.e., at 25 °C the uncertainty is 0.15 °C) with a repeatability of ± 0.05 °C. The pressure signal is produced from a commercial variable-capacitance type pressure transducer with an inaccuracy stated by the manufacturer (traceable to NIST) within 0.05% full scale and a repeatability within 0.01% full scale. Two commercial solar-blind ultraviolet sensitive vacuum phototubes, and amplifiers provide the detector signals.

Logic and time base circuitry provides the interaction between the electronics module and three 8-bit ports on a digital I/O card inside the control computer. A crystal oscillator and associated circuits produce the necessary 5-s timing sequence for the scalars used to obtain the correct temperature and pressure measurements. Ratios of the two optical channel frequencies are taken so that uncertainties in the time measurement do not significantly affect the accuracy of the transmittance measurement.

6. GAS FLOW and OZONE GENERATION

The gas flow and ozone generation system used in the SRP is outlined in Figure 3. The SRP requires a supply of reference air for operation. The supply of reference air entering the pneumatics module is split into two directions. A portion goes through a capillary tube and then to a manifold providing a supply of approximately 7 L/min of reference air. Another portion goes through a mass flow controller, the ozone generation unit, and then to a manifold providing the ozonized sample air. The ozone generation unit consists of a low pressure mercury lamp enclosed within a temperature controlled aluminum block. In the generation unit, ozone is produced by the photolysis of oxygen in a stream of reference air by ultraviolet radiation. The concentration of ozone in the air stream is dependent on the power level at which the lamp is operated and on the duration of exposure of reference air to the lamp (i.e., the residence time in the chamber as determined by the flow rate of air through the system). Lamp power is controlled by using an adjustable, high-frequency AC high-voltage current source which provides a highly stable lamp current in the range of 1.6 to 16 mA. Lamp temperature is stabilized by heating the aluminum block to a fixed temperature maintained within $\pm 0.1^\circ\text{C}$ using a commercial temperature controller. The flow rate of zero air through the generator is maintained by using a mass flow controller capable of providing a range of flows from 2 to 10 L/min. The flow rate of air and the lamp intensity are controlled by potentiometers on the front panel of the pneumatics module. A dual diaphragm pump pulls the sample and reference gases through the absorption cells at approximately 2 L/min while a pair of solenoid valves directs the sample to either cell.

7. MATERIALS and DIMENSIONS

The materials used throughout the gas sampling process of the SRP were chosen to minimize degradation of ozone in the sample air. The sample air passes through borosilicate glass manifolds, polytetrafluoroethylene transfer tubing, and borosilicate glass optical absorption cells. The solenoid valves, also made using polytetrafluoroethylene, were selected for low power operation to minimize sample heating. The temperature and pressure transducers are placed at an absorption cell exit to minimize decomposition of ozone in the sample during the measurement.

The path length through the absorption cells is approximately 89.50 cm and varies from instrument to instrument. This length was governed by the desire to transport the instrument, in a suitably padded shipping container, as checked baggage on commercial airlines. The cells have a 12 mm bore with a volume of approximately 100 mL. With a flow rate through the cells of approximately 2 L/min, the residence time for ozone in the cell is 3 seconds.

8. PHOTOMETRIC MEASUREMENTS WITH THE SRP

The ozone concentration, c , is calculated from the expression:

$$c = \frac{-\ln T}{\alpha L} \quad [1]$$

T is the transmittance of the sample while the terms α (absorption coefficient) and L (pathlength) are fixed quantities with known uncertainties. The commonly accepted value of α , $1.147 \times 10^{-17} \text{ cm}^2/\text{molecule}$ (or equivalently $308.32 \text{ atm}^{-1} \text{ cm}^{-1}$, base e) (3), is expressed at STP. The sample temperature and pressure are measured, and the sample concentration is corrected using the ideal gas law.

The optical layout of the SRP outlined in Figure 2 shows the four frequencies (detector 1, detector 2, temperature, and pressure) produced during each cycle of the measurement process. These frequencies are integrated over five second periods by counting the total number of digital pulses with counter circuitry. To determine the transmittance of the sample with high precision, the SRP is programmed to alternately flow the sample through one cell and reference air through the second cell, and then flow the sample through the second cell and reference air through the first cell.

The transmittance of the sample is calculated as the ratio I/I_0 where I and I_0 are the intensities of the UV radiation through the cells with and without ozone, respectively. The frequencies, or scaler count values, obtained during the first half-cycle of the instrument operation which correspond to I and I_0 are:

$$I = f_{11} = I_{11} K_1 f_{1nom} T_{1(cell1)} \quad [2]$$

$$I_0 = f_{21} = I_{21} K_2 f_{2nom} \quad [3]$$

I_{11} and I_{21} are apparent source strengths for the two optical channels. K_1 and K_2 are instrument constants that include such parameters as detector sensitivity, amplifier gain, and cell window transmittance which are assumed to stay constant from one instrument cycle to the next. f_{1nom} and f_{2nom} are the nominal frequencies of the two channels when the cells contain reference air. Finally, T_1 is the transmittance of the ozonized air in cell 1. The measured quantities for I_{11} and I_{21} are the electronic pulses from the detectors; their absolute values are not determined because they cancel out in the final ratio calculation. Similarly, during the second half-cycle, the frequencies which correspond to I and I_0 are:

$$I_0 = f_{12} = I_{12} K_1 f_{1nom} \quad [4]$$

$$I = f_{22} = I_{22} K_2 f_{2nom} T_{2(cell2)} \quad [5]$$

where $I_{12} = Q \times I_{11}$ and $I_{22} = Q \times I_{21}$ (the term Q accounts for the fact that the lamp intensity may change during an instrument cycle); and T_2 is the transmittance of the ozonized air in cell 2. After defining the minor ratios $r_1 = f_{11}/f_{21}$ and $r_2 = f_{12}/f_{22}$, the major ratio for the two half cycles is then defined a $T = r_1/r_2$. The full equation is then written as:

$$T = \frac{r_1}{r_2} = \frac{f_{11} f_{22}}{f_{21} f_{12}} = \frac{I_{11} K_1 f_{1nom} T_{1(cell1)} Q I_{21} K_2 f_{2nom} T_{2(cell2)}}{I_{21} K_2 f_{2nom} Q I_{11} K_1 f_{1nom}} \quad [6]$$

Upon canceling like terms: $T = T_{1(cell1)} T_{2(cell2)}$, where T is the transmittance of a sample of length equal to the length of cell 1 plus the length of cell 2.

The SRP system calculates T from the frequencies f_{11} , f_{12} , f_{21} , and f_{22} and the concentration is computed from equation 1. A temperature/pressure correction factor is then applied:

$$F = \frac{\text{sample temperature}}{\text{standard temperature}} \frac{\text{standard pressure}}{\text{sample pressure}} \quad [7]$$

which reduces the concentration to STP conditions, and finally the SRP's computer converts the concentration to ppbv.

To maximize the number of measurement points obtained per unit time, the instrument cycle can be extended by switching the system back to the flow configuration of the first "half-cycle" and obtaining a third minor ratio:

$$r_3 = \frac{f_{13}}{f_{23}} \quad [8]$$

This is then used in conjunction with the second minor ratio r_2 to obtain a second major ratio:

$$T_2 = \frac{r_3}{r_2} = T_{2(\text{cell}2)} T_{3(\text{cell}1)} \quad [9]$$

and a second, though not independent, measurement can be obtained in only 50 % more time than that required for a single measurement. A fourth minor ratio would then be defined as:

$$r_4 = \frac{f_{14}}{f_{24}} \quad [10]$$

Again this is used in conjunction with the previous minor ratio r_3 to obtain the third major ratio:

$$T_3 = \frac{r_3}{r_4} = T_{3(\text{cell}1)} T_{4(\text{cell}2)} \quad [11]$$

The instrument cycle can be extended for an arbitrary number of half-cycles. In practice, the system is typically programmed to obtain 7 to 10 measurements/concentration; one major ratio yields one measurement. The standard deviation of the set is calculated, and if it is within preset tolerances, the average value is taken for the concentration.

9. PERFORMANCE

A typical set of readings from the main NIST SRP measuring zero air in both cells is shown in Table 2. Column one lists the half cycle number, columns two and three contain the 5-s integrated count values that correspond to light intensities from the two optical cells, column four is the temperature, and column

five is the pressure for each period. Starting with half cycle one, column six lists the volume concentration of ozone in ppbv computed from the latest and previous half cycle data. In this run, the instrument zero level is determined from the ten half cycle measurements to give nine ozone concentration determinations.

A typical SRP calibration run is composed of ten ozone concentrations covering the range of 30 ppbv to 1000 ppbv measured in random order with an additional zero air level measured at the beginning and end of the run. A summary of the measurements for three of the twelve ozone concentrations for a typical calibration run is shown in Table 3. The values are tabulated in the relative order they were recorded to show time dependence of the parameters. The average value and standard deviation of the temperature and pressure are for ten half-cycle readings while the ozone concentration is for nine determinations during each measurement set. Table 3 also shows the change in measured counts between the two half cycles for optical cell 1. The cell 1 values are of the five even numbered half cycles when zero air is flowing through the cell. The Δ cell 1 averages and standard deviations are for five changes in the optical signal when ozone is in the cell (odd numbered half cycles). Similar values for cell 2 are not shown. The twelve ozone concentrations from a typical calibration run are fitted to a line by linear least-squares regression to determine the slope and intercept of the calibration function. A plot of the twelve recorded points for SRP-0 vs SRP-2 calibration run is shown in Figure 4a with the residuals (observed value minus fitted value) in Figure 4b.

Table 4 shows a series of typical comparisons between the two SRPs. Each comparison is similar to the run data shown in Figure 4 and consists of twelve concentration values; ten with ozone present and two with zero air present in the sample stream. The ten different calibration runs were conducted over the course of a month with SRP-0 turned off between some runs and transported by car to a user site for comparison with another instrument. SRP-2 was not turned off between calibration runs but left in a power ON standby state. Calibration runs on the same day were done consecutively. The first two columns contain the number and date of run. The next two pairs of columns contain the values and standard deviations for the slopes and intercepts of the fitted straight lines. The Rsq column contains the correlation coefficient for the linear regression. The last column, RSD, is the standard deviation of the residuals. The last two rows show the average and standard deviation of the values in the corresponding columns.

10. ANALYSIS OF PERFORMANCE

The SRP was designed with a single analyzer light source, twin sample cells, simultaneous counting, minor and major ratios, and other features to reduce many of the sources of noise inherent in absorption detectors. Close examination of the SRP performance data shows the effectiveness of the design at reducing uncertainties in the measured ozone concentration. The following inspection of the data, as a function of ozone concentration, time, and half cycles, gives a revealing look into the operation of the instrument.

Table 2 shows the light signals in the two optical cells have comparable but not identical values. The average and standard deviation (in parentheses) of optical cells 1 and 2 are 73304.6 (4.4) and 73568.0 (4.9), respectively, for reference air. The average value and standard deviation of the minor ratio for the ten half cycles are 1.003593 and 0.000012, respectively. If one assumes the observed variation in the optical signals from the two channels are random and uncorrelated, then the estimated value for the

standard uncertainty of the minor ratio is 0.000089. This value is over seven times larger than observed and illustrates that ratios of the two channels reduces the effects of correlated noise due to lamp variations.

Counting noise limits the precision of the calculated minor ratios. Counters operating in a non-synchronous mode can be biased by at most $\frac{1}{2}$ count. Assuming that any value in the range of $\pm \frac{1}{2}$ count is equally likely, the standard uncertainty (4) is given by²:

$$\frac{0.5}{\sqrt{3}} = 0.29 \quad [12]$$

Using 0.29 as the standard uncertainty along with the data in Table 2 gives a computed standard uncertainty in the minor ratio of 0.000006. Compared with the experimental value of 0.000012 computed from the data in Table 2, the SRP approaches the counting noise limit and in some measurement sets actually reaches this limit. The effect of counting is that the finite resolution in the counts produces discrete levels, which is apparent in the ozone concentration levels shown in Table 2.

Analysis of the minor ratios only shows the reduction in optical signal variation during a particular half cycle. On alternating half cycles each cell measures reference air, then air with ozone. The cell 1 and Δ cell 1 rows in Table 3 show the effect of this changing stream on the detected optical signal. The standard deviation of the Δ cell 1 measurements is less than that of cell 1 values. The contrast is even greater when one considers that the difference calculations require two count measurements resulting in a delta that should have a standard uncertainty $\sqrt{2}$ times higher than the cell standard uncertainty. The optical detection system shows a small drift in lamp intensity evident by the increasing cell counts of Table 2 and the cell counts for the three different ozone concentrations of Table 3. The repeating of alternate half cycles removes much of the variation due to source lamp intensity drifts.

The Δ cell 1 values in Table 3 indicate that changes in the transmitted light are small; at most about 2.5% at high concentrations (998 ppbv) and 0.4% at low concentrations (165 ppbv). The standard uncertainties of the high and low cell count values include ozone generator fluctuations while the reference air values are mainly due to lamp variations. The ozone generator variations are evident in the standard uncertainty of the average ozone concentrations calculated for each measurement set. All standard uncertainties are low, but show a slight increase with concentration (0.27 vs 0.50 ppbv at concentrations of 0.2 and 997.6 ppbv, respectively).

The temperature and pressure readings in Table 3 show constant values for a calibration run with very small standard deviations. Close examination of the temperature and pressure measurements in the odd and even numbered half cycles of Table 2 reveals a slight asymmetry in the temperature (0.02 °C) and pressure (0.47 mbar). These small differences are constants for each instrument. The major contributors to the standard deviation of the temperature are differences between the odd and even half cycles and a slight increase in the room temperature as a function of time. Similarly for the measured pressure, the

² The square root of three is used following the rules of uncertainty analysis for an interval with uniform probability.

standard deviation for a measurement set is small but dominated by the pressure difference in the half cycles with (in this run) a very small pressure drop over time. The time dependences of pressure and temperature are highly correlated between different instruments in a calibration run and are due to changes in the surrounding laboratory environment.

The reproducibility of the calibration curves is evident by the values listed in Table 4. The slope of the calibration line is 1.00003 with a relative standard uncertainty of about 0.06%. The intercept varies slightly, but on average is not statistically different from zero. The correlation coefficients (Rsq) give some indication of how well the calibration curve is represented by a linear relationship between the two SRPs and is typically in the six “nines” (0.999999) range. The linearity of the calibration curves is obvious in figure 4 where the deviations from a straight line are only visible in the residual plot and have a maximum/minimum of ± 0.5 ppbv. The RSDs in Table 4 show the difference between the observed SRP-0 values and the fitted line and are, on average, only a few tenths of a ppbv. Overall, Table 4 shows a very consistent operation over time and an absence of outliers.

11. MEASUREMENT UNCERTAINTIES

The performance analysis of the SRP just presented can only quantify the precision of the instrument and cannot directly yield a measure of accuracy. Provided there are no unknown biases or sources of error in the SRP, the uncertainty in the accuracy can be determined by evaluating the effects of uncertainty in temperature, pressure, cell length, cell counts, and absorption coefficient on the ozone concentration calculated from equation numbers 1, 6, and 8.

Application of the law of propagation of uncertainties to equations that involve only multiplication or division shows that the total uncertainty is a combination of the relative fractional uncertainties in each quantity. The relative uncertainties are combined vectorially, that is, taking the positive square root of the sum of the squared component uncertainties. The uncertainty of the transmittance (major ratio) is derived from the uncertainties in the four optical frequencies from two half cycles. Taking twice³ the counting noise ($2 \times 0.29 = 0.58$ counts) as the uncertainty in a single optical measurement leads to an uncertainty in the transmittance of 0.000017 and is nearly constant for the entire measurement range of the SRP. The relative uncertainty in the concentration of ozone ($\delta c/c$) as a function of transmittance can be derived from equation 1 to give:

$$\frac{\delta c}{c} = \frac{\delta T}{T \ln(T)} \quad [13]$$

where δT is the uncertainty in transmittance. Table 5 shows the range of transmittance values corresponding roughly to the operating range of the SRP along with the absolute and relative uncertainties in ozone concentrations. As noted earlier, the uncertainty in transmittance is nearly constant, and is assumed constant for calculations in the table. The uncertainty in transmittance leads to a nearly constant absolute uncertainty in the concentration of ozone, resulting in a large relative uncertainty at low concentrations and a very low uncertainty at the upper limit of the instrument.

³ Coverage factor of 2 standard deviations is used for all expanded uncertainty values.

The absorption coefficient (α) has a stated range of 2 %, or ± 1 % (3). Assuming each value in this range is equally likely, then the relative standard uncertainty is found (as in the counting noise described earlier) by dividing by $\sqrt{3}$ to give 0.58 %. The relative standard uncertainty in the path length is derived from the shortest SRP cell length of 89.25 ± 0.05 cm to give 0.033 %. The standard uncertainty of the temperature at 25 °C (298.15 K) is 0.15 °C to produce a relative standard uncertainty of 0.029 %. The pressure transducer has a stated standard uncertainty of 0.05 %. This corresponds to 0.029 kPa assuming a uniform probability of being in this range, as in the cases of temperature and counting noise, and is comparable with the observed standard deviation in the pressure of 0.032 kPa (0.24 torr) mainly due to pressure differences in the half cycles. Taking a value of 0.030 kPa for the standard uncertainty in pressure yields a relative standard uncertainty of 0.03 %.

Table 6 shows a summary of the contribution of the various measurements to the uncertainty in concentration of ozone. Uncertainties in temperature, pressure, and path length all have minimal impact on the combined uncertainty in the concentration of ozone. The determination of transmittance has a variable contribution to the combined uncertainty of the ozone measurement but is only significant below about 100 ppbv. Table 6 clearly shows that the accuracy of the ozone concentration measurements is dependent largely upon the uncertainty in the absorption cross section value used in the SRP calculations.

12. CONCLUSIONS

The dual absorption cell design of the SRP inherently reduces systematic biases and drift effects. The major source of uncertainty in the measured ozone concentrations is the uncertainty in the absorption cross-section at 254 nm. Comparisons between two SRPs demonstrates a precision better than the calculated absolute uncertainty. The evaluation of absolute uncertainty is based on the assumption that no systematic biases are present. The SRP is currently undergoing an exhaustive evaluation of systematic errors, which will be the subject of a future report.

In concluding remarks, data from the entire SRP network (not presented here) have indicated that the SRP is a reliable and repeatable ozone standard calibration instrument. Intercomparisons conducted annually over the last decade have shown the SRPs to be in agreement to better than 0.5 % over the concentration range 100 ppbv to 1000 ppbv and ± 1 ppbv over the concentration range 0 ppbv to 100 ppbv. This network has met the needs of the user community responsible for ozone calibration by providing local access to authoritative ozone standards.

13. ACKNOWLEDGEMENTS

We are indebted to Mr. Larry Purdue, Senior Scientist (retired), Human Exposure and Field Research Division, Atmospheric Research and Exposure Assessment Laboratory, EPA/RTP, for support of the development of the Standard Reference Photometer described in this paper.

The surviving authors would like to pay tribute to the memory of Dr. Arnold M. Bass. After a long illustrious career, Dr. Bass died of cancer at age 66 on March 21, 1989. Dr. Bass graduated from the College of the City of New York in his native New York City. He then received a masters degree and a doctorate in physics from Duke University. After two years of post doctoral study at the Massachusetts Institute of Technology, Dr. Bass joined the then National Bureau of Standards in 1950. During his

career at NBS, he served as staff physicist, deputy chief of the Free Radical Research Section, deputy chief of the Physical Chemistry Division, and ended his career as senior scientist in the Center for Analytical Chemistry. In his scientific career, Dr. Bass was internationally known for his work in the ultraviolet spectroscopy of small gaseous molecules. He was best known for his collaborative efforts with Dr. Richard J. Paur of the Army Research Office in the areas of temperature dependent spectral cross sections of the ozone molecule at stratospheric temperatures and the development of the national primary standard for atmospheric ozone concentrations based on ultraviolet photometry. Survivors include his wife of 41 years, Rosalyn Bass, three sons, Dr. Jonathan Bass, Dr. David Bass, and Daniel Bass, and a sister, Helen Gurin.

14. REFERENCES

1. Title 40 of the *Code of Federal Regulations*, Part 50, Appendix D (40 CFR Part 50).
2. Proffitt, M.H., McLaughlin, R.J., Fast-Response Dual-Beam UV-Absorption Ozone Photometer Suitable for use on Stratospheric Balloons, *Review of Scientific Instrumentation (USA)*, Volume 54, Number 12, December 1983.
3. Demore, W.B., Sander, S.P., Golden, D.M., Molina, M.J., Hampson, R.F., Kurylo, M.J., Howard, C.J., Ravishankara, A.R., *Chemical Kinetics and Photochemical Data for Use in Stratospheric Modeling*, Evaluation Number 11, JPL Publication 94-26, Jet Propulsion Laboratory, Pasadena, California, USA.
4. Taylor, Barry N. and Kuyatt, Chris E., "Guidelines for Evaluating and Expressing the Uncertainty of NIST Measurement Results," *National Institute of Standards and Technology Technical Note 1297*, 1994 Edition (U.S. Government Printing Office, Washington, D.C., September 1994).

Table 1. Specific Locations of Standard Reference Photometers

<u>SRP#</u>	<u>Completion Date</u>	<u>Location</u>	<u>Organization</u>
0	August 1985	Gaithersburg, MD	NIST (2)
1	February 1983	Research Triangle Park, NC	U.S. EPA ORD
2	February 1983	Gaithersburg, MD	NIST (1)
3	August 1983	Edison, NJ	U.S. EPA Region II
4	September 1983	Sacramento, CA	U.S. EPA Region IX
5	March 1985	Houston, TX	U.S. EPA Region VI
6	March 1985	Chicago, IL	U.S. EPA Region V
7	January 1986	Las Vegas, NV	U.S. EPA R&IE (Main)
8	February 1986	Denver, CO	U.S. EPA Region VIII
9	May 1987	Lexington, MA	U.S. EPA Region I
10	November 1987	Athens, GA	U.S. EPA Region IV
11	September 1987	Stockholm, Sweden	Institute of Applied Environmental Research
12	July 1988	Toronto, Canada	Ontario Ministry of Environment
13	January 1989	Kansas City, KS	U.S. EPA Region VII
14	June 1993	Bern, Switzerland	Swiss Federal Office of Metrology (1)
15	October 1993	Dübendorf, Switzerland	Swiss Federal Laboratories for Materials Testing and Research (1)
16	October 1994	Ottawa, Canada	Environment Canada
17	December 1994	Prague, Czech Republic	Czech Hydrometeorological Institute
18	January 1996	Bern, Switzerland	Swiss Federal Office of Metrology (2)
19	November 1996	Braunschweig, Germany	Physikalisch-Technische Bundesanstalt
20	March 1997	London, United Kingdom	National Physical Laboratory
21	June 1997	Sydney, Australia	NSW-Environment Protection Authority
22	December 1997	Madrid, Spain	Instituto de Salud Carlos III
23	March 1999	Dübendorf, Switzerland	Swiss Federal Laboratories for Materials Testing and Research (2)
24	February 2000	Paris, France	Laboratoire National D'Essais
25	June 2001	Lisbon, Portugal	Direcção Geral Do Ambiente
26	December 2001	Vienna, Austria	Umweltbundesamt
27	April 2002	Sèvres, France	Bureau International des Poids et Mesures (1)
28	April 2002	Sèvres, France	Bureau International des Poids et Mesures (2)
29	June 2002	Langen, Germany	Umweltbundesamt
30	November 2002	Kaohsiung, Taiwan R.O.C.	Taiwan Environment Protection Administration

Table 2. Tabulated data for a typical zero air measurement of a calibration run. Ten half cycles are completed to produce nine replicate ozone concentration measurements. The significant figures in the temperature and pressure columns do not imply measurement accuracy but only show the precision of the instrument.

Half Cycle Number	Cell 1 (count)	Cell 2 (count)	Temp. (°C)	Press. (mbar)	[O ₃] (ppbv)
0	73300	73563	24.017	992.71	
1	73300	73562	24.037	992.23	-0.3
2	73301	73563	24.019	992.63	0.0
3	73299	73563	24.042	992.19	0.5
4	73303	73566	24.022	992.64	0.3
5	73306	73571	24.044	992.20	0.5
6	73308	73571	24.024	992.68	0.5
7	73307	73571	24.042	992.15	0.3
8	73311	73575	24.025	992.68	0.0
9	73311	73575	24.044	992.21	0.0

Table 3. Average value and standard deviation of measured parameters for three different ozone concentrations: zero, low, and high. The values given for the zero ozone level one are for the data in Table 2. The three levels are shown in the relative order that they were collected.

	Ozone Level					
	Zero		High		Low	
Parameter	Average	Std. Dev.	Average	Std. Dev.	Average	Std. Dev.
Cell 1 (counts)	73304.6	4.2	73279.0	7.1	73267.0	3.9
Δ Cell 1 (counts)	0.0	2.0	-1795.0	4.0	-297.8	3.0
Temperature ($^{\circ}$ C)	24.032	0.011	24.070	0.010	24.096	0.009
Pressure (mbar)	992.43	0.24	992.21	0.24	992.07	0.26
[O ₃] (ppbv)	0.20	0.27	997.64	0.50	165.30	0.28

Table 4. Multiple comparisons of calibration runs for SRP-0 vs SRP-2.

Run	Date	Slope	Std. Dev.	Intercept	Std. Dev.	Rsq	RSD
OZN8127	01-Aug	0.99897	0.00032	-0.197	0.091	0.9999990	0.378
OZN8128	03-Aug	1.00007	0.00021	-0.364	0.148	0.9999996	0.249
OZN8129	03-Aug	0.99997	0.00023	-0.275	0.115	0.9999995	0.275
OZN8133	20-Aug	1.00041	0.00036	-0.239	0.111	0.9999987	0.421
OZN8134	20-Aug	0.99996	0.00024	-0.002	0.035	0.9999994	0.279
OZN8135	21-Aug	1.00026	0.00023	0.077	0.046	0.9999995	0.264
OZN8138	26-Aug	1.00071	0.00023	-0.009	0.034	0.9999995	0.265
OZN8139	27-Aug	1.00073	0.00020	-0.248	0.107	0.9999996	0.235
OZN8140	27-Aug	1.00013	0.00022	-0.048	0.038	0.9999995	0.260
OZN8141	29-Aug	0.99910	0.00018	-0.003	0.027	0.9999997	0.214
Average		1.00003	0.00024	-0.131	0.075	0.9999994	0.284
Std. Dev.		0.00056	0.00005	0.142	0.042	0.0000003	0.061

Table 5. Relationship of expanded uncertainty (U) in transmittance to the absolute and relative U in the calculated ozone concentration. U is assumed to be 0.000017.

Trans.	[O ₃] (ppbv)	[O ₃] U (ppbv)	relative U (%)
0.9999	1.82	0.31	17
0.9990	18.18	0.31	1.7
0.9950	91.08	0.31	0.34
0.9700	553.45	0.32	0.057
0.9450	1027.90	0.33	0.032

Table 6. Comparison of the sources of uncertainty and their relative contribution to the uncertainty in the measured ozone concentration of the SRP.

Measurement	Expanded Uncertainty	Relative Uncertainty (%)	Relative Uncertainty in [O ₃] (%)
Absorption Coefficient 1.147x10 ⁻¹⁹ (cm ² /molecule)	1.0%	0.58	0.58
Transmittance	0.000017	0.0017	0.057
Pressure	0.03 kPa	0.03	0.03
Temperature	0.15 °C	0.029	0.029
Path Length	0.05 cm	0.033	0.033

a) Values for transmittance are taken at an [O₃] of 553 ppbv.

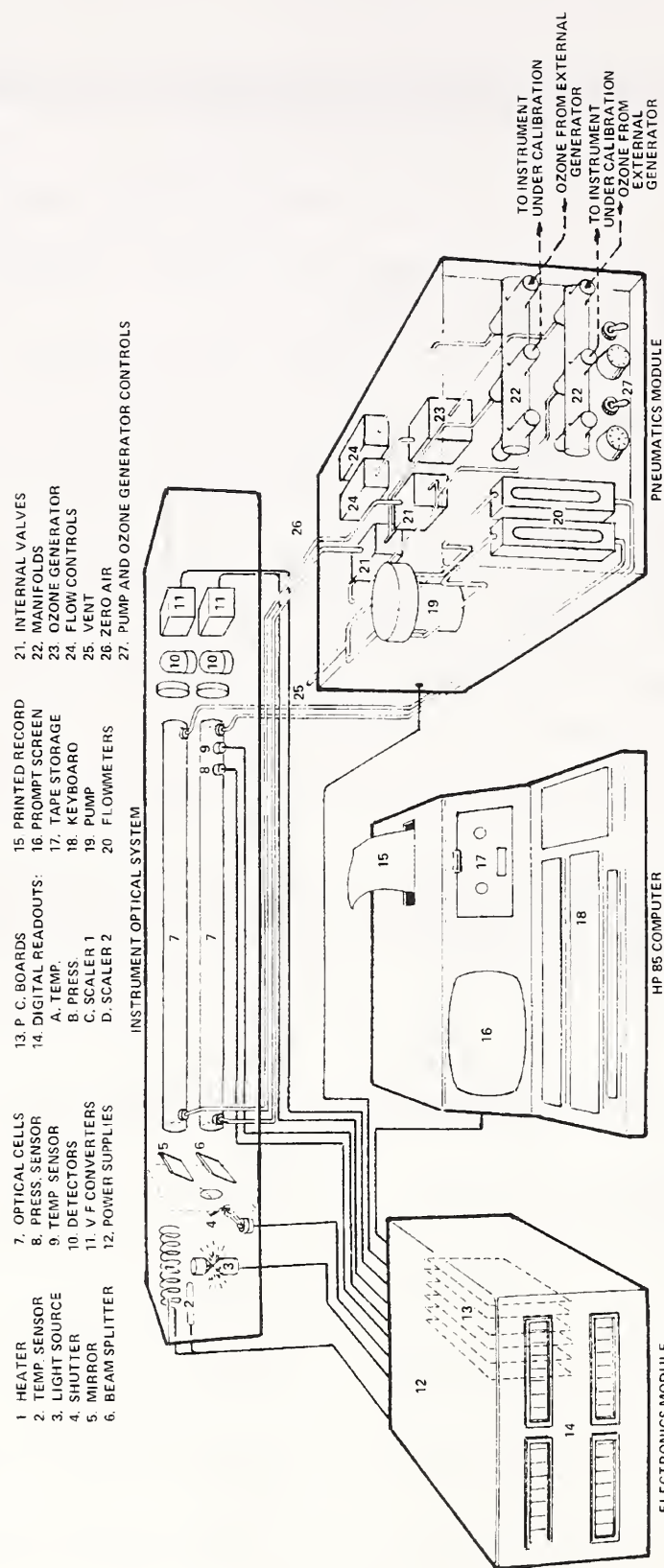


Figure 1. Layout of the Standard Reference Photometer with original computer.

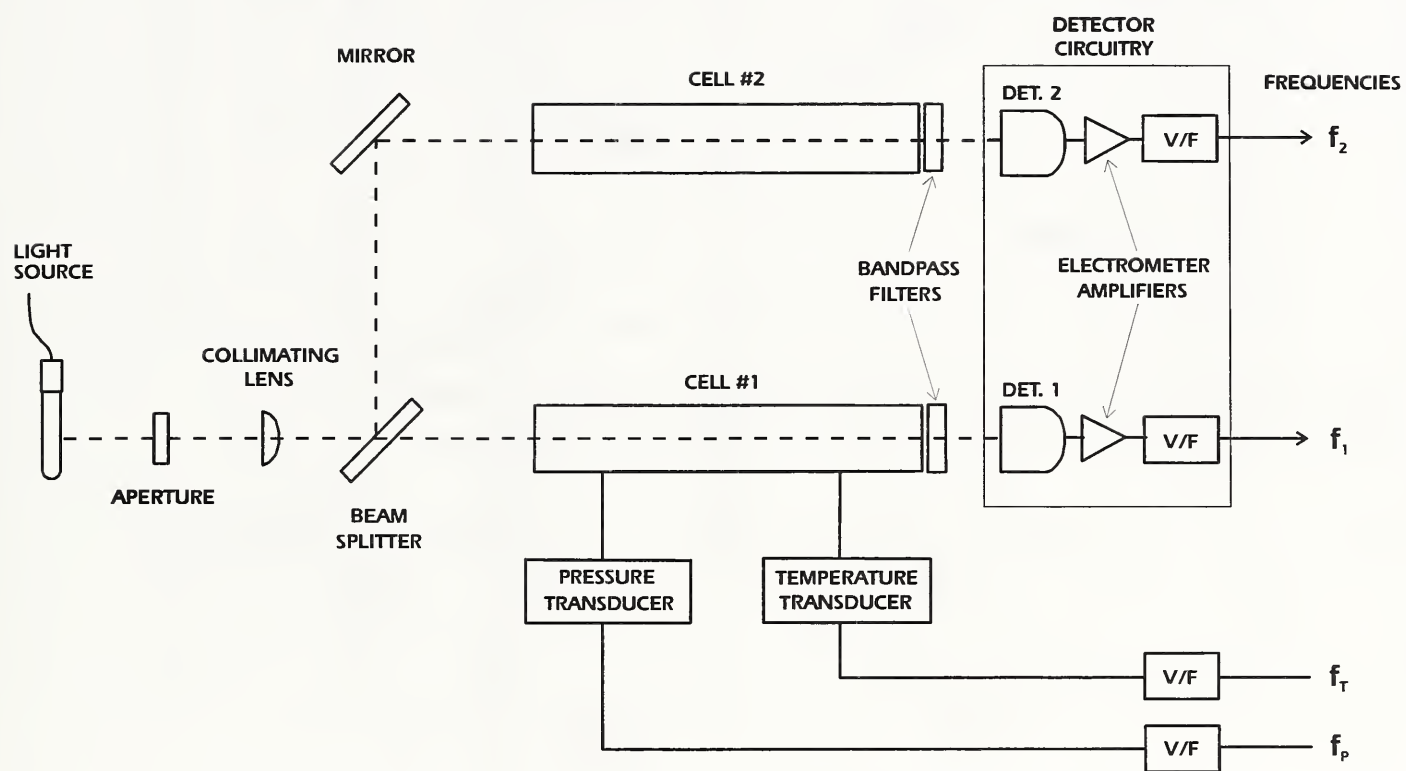


Figure 2. Optical Layout of the SRP.

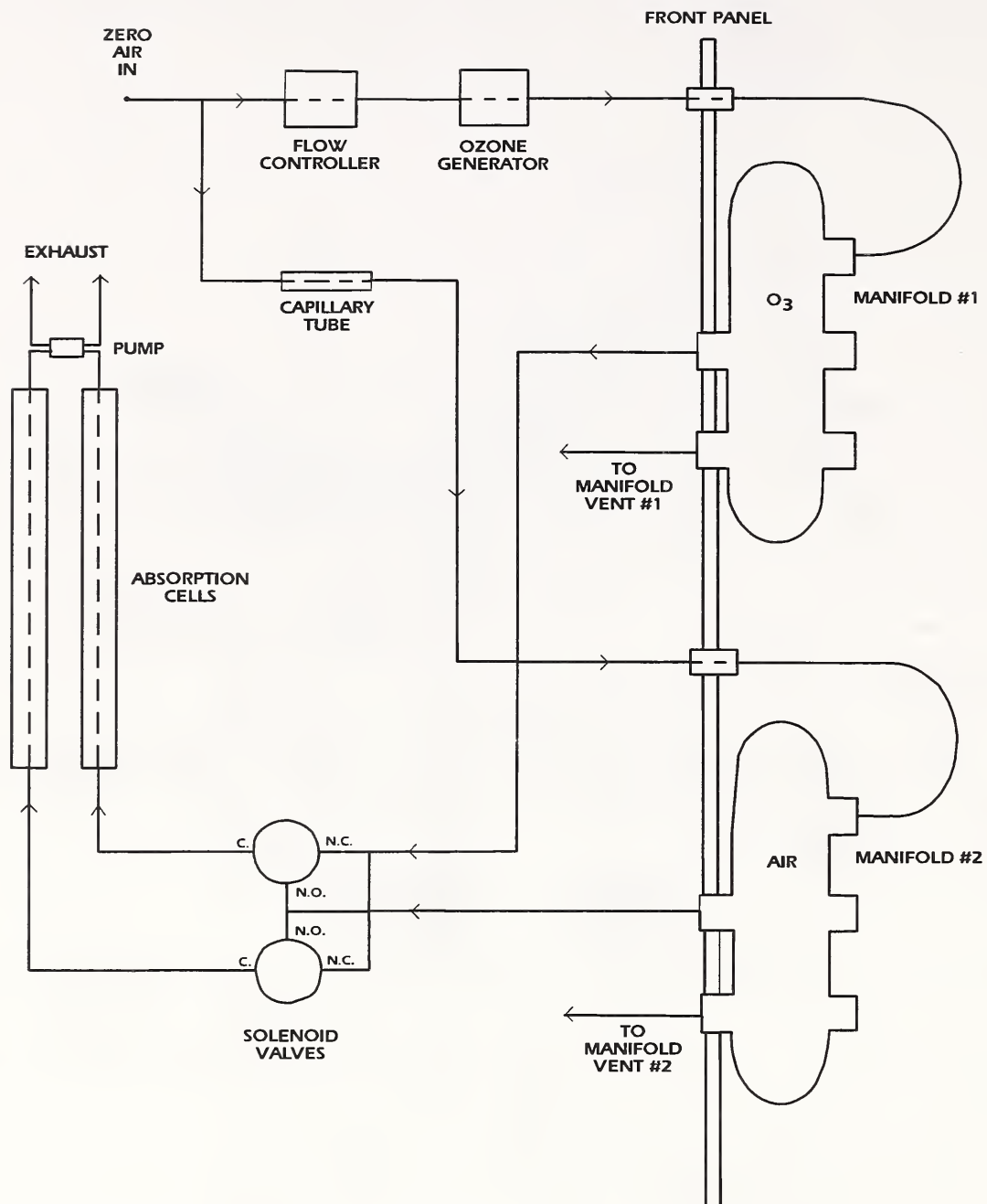


Figure 3. SRP Flow Schematic

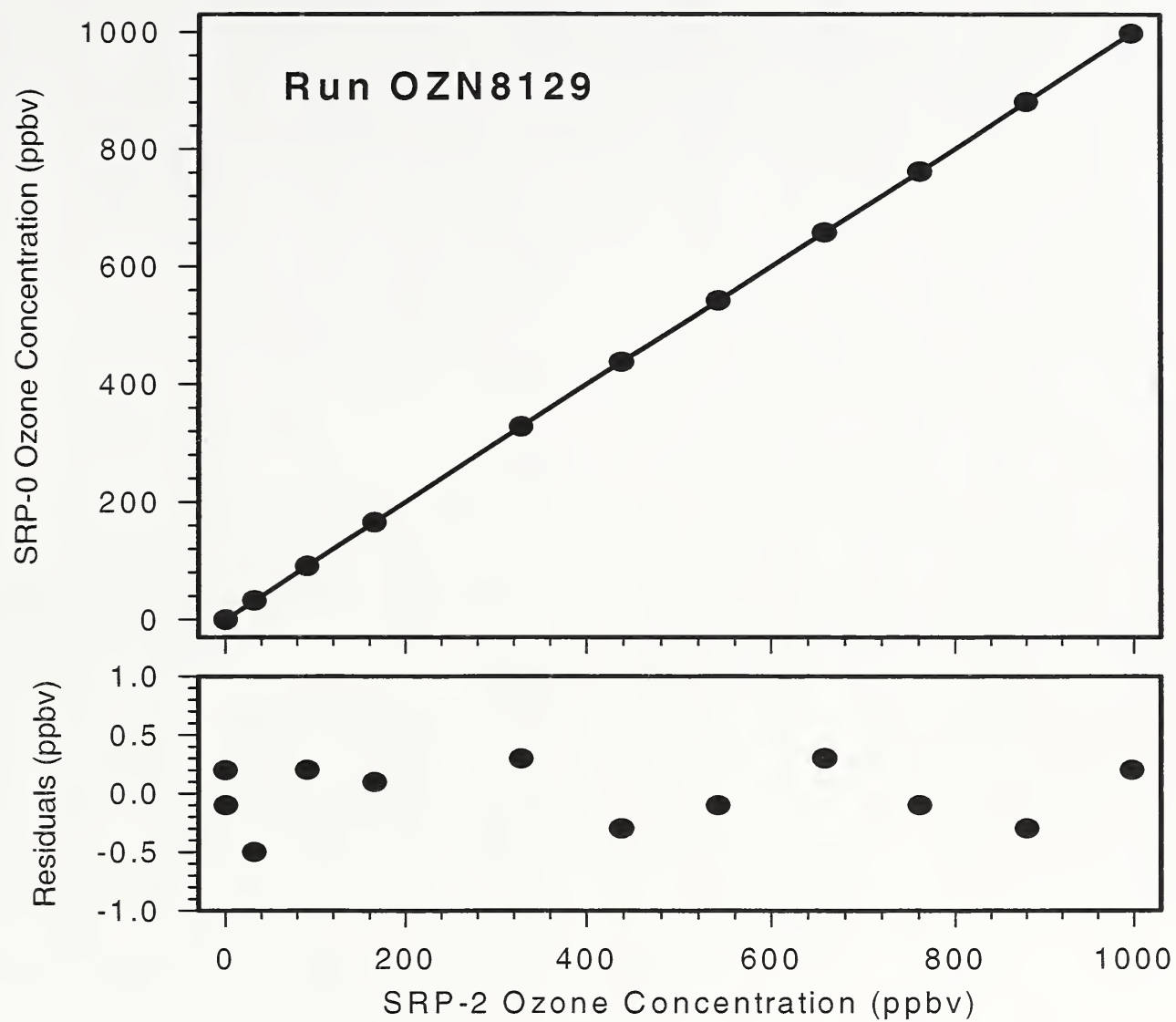


Figure 4. Plots of the calibration line (a) and the residuals (b) for the two NIST SRPs.

